SCIENTIFIC PAPER
Published: June 12, 2025
https://doi.org/10.13167/2025.30.16

Analytical estimation of fundamental periods of coupled systems

Omid Fereidooni[1], Panam Zarfam[1] and Mohammadreza Mansoori[1]

[1] *Department of Civil Engineering, Science and Research Branch, Islamic Azad University, Tehran, Iran*

Corresponding author:
Panam Zarfam
zarfam@srbiau.ac.ir

Received:
October 13, 2024

Revised:
March 18, 2025

Accepted:
March 26, 2025

Published:
June 12, 2025

Citation:
Fereidooni, O.; Zarfam, P.; Mansoori, M.
Analytical estimation of fundamental periods of coupled systems.
Advances in Civil and Architectural Engineering,
2025, 16 (30), pp. 287-306.
https://doi.org/10.13167/2025.30.16

ADVANCES IN CIVIL AND ARCHITECTURAL ENGINEERING (ISSN 2975-3848)

Faculty of Civil Engineering and Architecture Osijek
Josip Juraj Strossmayer University of Osijek
Vladimira Preloga 3
31000 Osijek
CROATIA

Abstract:
This study provides an in-depth analytical investigation to accurately estimate the seismic responses of coupled systems while considering primary–secondary system interactions (PSSIs). A practical modal analysis-based approach was proposed to estimate the fundamental period of multi degrees-of-freedom (MDOF) steel moment-resisting frame structures. A follow-up numerical investigation was performed to successfully verify the results obtained from the proposed relationship. Subsequently, the effects of the secondary system multiplicity, number of frame storeys, mass ratio, and distribution of secondary systems along the frame height were assessed on the fundamental period of the coupled system. Based on the results, the seismic response of the short-period coupled systems was improved by increasing the period of the overall system under the effect of the secondary structure period. The findings of this study confirm that the presence of multiple secondary structures significantly influences the fundamental period of a coupled system when PSSI effects are considered. In contrast to current design code recommendations, it was found that the total mass of the secondary structures cannot be ignored in calculations owing to the multiplicity of secondary systems.

Keywords:
fundamental period; modal analysis; primary–secondary system interaction (PSSI); moment-resisting frame; mass ratio; multiplicity

1 Introduction

Several studies have examined the interactions between the primary and secondary systems in coupled structures [1-5]. The computational complexity of these studies is such that it is practically impossible to use them as design techniques. Therefore, simplified methods for coupled system analysis and design have been proposed [6-8]. Adam [9] experimentally investigated the behaviours of secondary systems. We focused on the responses of the structures when the secondary structure frequency was close to the primary structure frequency. Filiatrault et al. [10] showed that the performance level of coupled structures is low because of the damage or collapse of nonstructural components, which is not admissible in vital infrastructures. Accordingly, the development of experimental research has been emphasised. A simple floor response spectrum (FRS) method for analysing the responses of nonstructural equipment has been proposed [11-12]. This method estimates the maximum response of the secondary system using the response spectrum obtained from the response of the primary structure. Kazantzi et al. [13] studied strength reduction factors for designing light nonstructural elements and provided approximate equations for estimating system responses. Chalarcal et al. [14] studied the seismic demand for acceleration-sensitive nonstructural components in braced frames.

Numerous studies have claimed that the fundamental period of a structure is the key parameter affecting its seismic behaviour. The accurate determination of this parameter helps correctly predict the seismic behaviour of the structure. In recent years, several researchers have proposed accurate methods for determining the fundamental periods of various structures under different conditions [15-18]. It is clear that the fundamental period of the primary structure changes with the addition of secondary systems. However, the alteration of the fundamental periods of primary structures has not received sufficient attention in previous studies; thus, limited research has been conducted on the periods of structures considering infill walls [19-20]. Neglecting this issue can cause computational errors when predicting the seismic behaviours of secondary and coupled structures. The effects of the fundamental periods on the seismic performance of base-isolated multistorey buildings were thoroughly investigated by Pandian and Vinu [21].

A review of previous research implies that secondary systems are always considered detrimental and threatening to the safety of structures. Thus, considering their seismic behaviour has been a priority in recent research. In contrast, owing to the complexity of primary–secondary system interaction (PSSI) relationships, developing design techniques based on simplified assumptions is necessary. The elimination of PSSI and assumption of the independent behaviour of the primary and secondary systems have been the most used in relevant research, especially regarding the relationships developed in seismic codes. In this hypothesis, the secondary system is assumed to be a single independent system with a small mass; therefore, the issue of the multiplicity of secondary systems has received little attention because of the elimination of the PSSI. However, the multiplicity of the secondary systems in the structure and their relatively significant total masses can be considered as structural seismic behaviour control parameters. The minimal application involves increasing the period of the coupled system and improving its seismic behaviour by reducing the seismic base acceleration of the coupled structure. Because a simple and practical technique has not been proposed for calculating the fundamental period of a coupled system, efforts have been made to create conditions for the non-interference of the primary and secondary structures. In contrast, the effects of secondary systems on the seismic behaviour of coupled structures have been neglected. In addition, structural engineers are uncertain about changes in the primary structure behaviour under the influence of secondary systems because of the small mass of each secondary system (alone) compared with the mass of the primary structure. Moreover, interaction effects are more likely to be ignored when the primary structure is affected by secondary systems.

Furthermore, it is common practice for structures to include masonry infill walls with openings, such as doors and/or windows. For example, Asteris [22] investigated the influence of a masonry infill panel opening on the reduction in multistorey and fully or partially infilled frame stiffness and concluded that the redistribution of the shear force was critically influenced by the presence and continuity of the infill panels. Thus, an increase in the opening percentage led to a decrease in the lateral stiffness of the infilled frames. In another study, Yekrangnia and Asteris [23] proposed a multi-strut macro-model to simulate the force–displacement behaviour of infilled frames with various opening configurations. They introduced a simple reduction factor for the ultimate strength of perforated infilled frames based on the opening size, relative to the infill wall size as well as the relative stiffness of the frame and infill wall.

This paper presents an analytical approach to the studied models. Subsequently, the numerical modelling of the frame systems is explained. Next, the periods of the coupled systems resulting from the combination of single-degree-of-freedom primary and secondary systems are discussed based on the results obtained via both numerical modelling and the proposed analytical relationship.

Thus far, either the period or the frequency of the structure has been considered as a complementary parameter in the current technical literature for calculating system responses and equations of motion. Thus, these parameters have been neglected, as the responses of the secondary and primary systems are typically assumed to be independent, given that the mass of the secondary system is negligible compared with that of the primary system. However, the present study highlights the effect of the secondary system on the response of the coupled system in the design procedure, with the period being the most evident of them. Owing to the multiplicity of the secondary systems, it is assumed that the total mass of the secondary systems cannot be ignored in the calculations. Furthermore, the proposed approach has the advantage of modifying the periods of primary structures with shorter periods, such that the coupled structure would benefit from increased period values by using the potential of multiple secondary systems. Thus, the behaviour of the entire structure can be improved seismically.

2 Methodology

2.1 Analytical approach

This section describes the configurations of the models examined in this study. A number of three-dimensional (3D) steel moment-resisting frame structures with one, two, and three storeys, each of which consists of four perimeter columns and four perimeter beams on each storey, were selected as primary systems, as illustrated in Figure 1. The detailed specifications of the selected frames are discussed below. The dimensions and weights of the frames were chosen such that the period of the initial structures was in the range of 0,15-0,70.

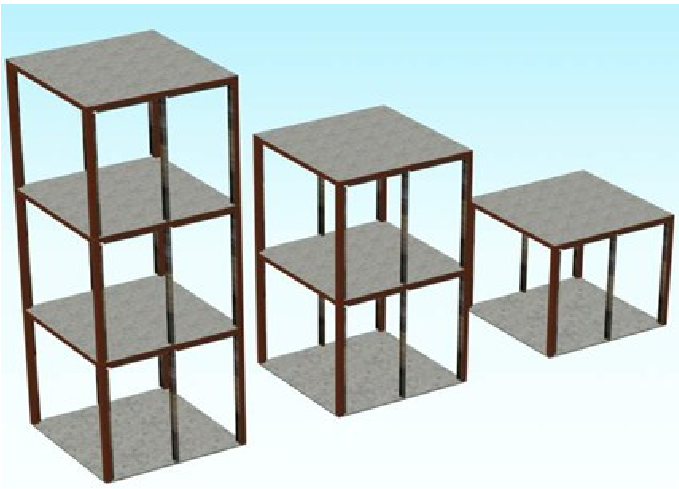

Figure 1. Schematic of the coupled frame structure

The results of preliminary investigations by the authors indicated that the most influential parameter in determining the responses of coupled systems was the period of these systems in relation to the fundamental period of the primary structure. In this regard, the behaviour of the coupled system can be characterised, given that the corresponding system period is known. Thus, the dynamic relationships of the coupled systems were investigated to estimate the period of the coupled system within an acceptable margin of error by proposing an appropriate formulation. Notably, general relations are first presented in the development of secondary system relations. Subsequently, a simplified relation is proposed as a design technique for estimating the period of the coupled system by using a series of simplifying assumptions.

The mass and stiffness matrices must be determined to calculate the fundamental period of the coupled system, and its characteristic equation must be calculated. Other researchers have performed this process for secondary systems, and this process will be extended using a similar approach to that for the multiplicity of secondary systems. Moreover, the indices *p*, *s*, and *c* have been used to define the characteristics of primary, secondary, and coupled systems, respectively. Moreover, the index *i* was used to indicate the degrees of freedom of the primary system, and the index *j* indicates the secondary system number.

Accordingly, the mass and stiffness of each single-degree-of-freedom (SDOF) are determined by m$s\ ij$ and k$s\ ij$, respectively, which denotes the mass and stiffness of the *j*-th secondary system, connected to the *i*-th degree of freedom in the primary system.

We assume that m SDOF secondary systems are connected to different degrees of freedom of a primary system with n DOF. The mass and stiffness matrices of the primary system are denoted by $[Mp]$ and $[Kp]$, and the mass and stiffness matrices of the coupled system are denoted by $[Mc]$ and $[Kc]$, respectively.

$$[M_c] = \begin{bmatrix} [M_{pp}]_{n*n} & [M_{ps}]_{n*m} \\ [M_{sp}]_{m*n} & [M_{ss}]_{m*m} \end{bmatrix}$$
$$[K_c] = \begin{bmatrix} [K_{pp}]_{n*n} & [K_{ps}]_{n*m} \\ [K_{sp}]_{m*n} & [K_{ss}]_{m*m} \end{bmatrix} \tag{1}$$

The mass and stiffness matrices in Equation (1) are expressed in Equations (2) and (3), respectively:

$$[M_{pp}] = [M_p] \ \ \& \ \ [M_{ps}] = [M_{sp}] = 0$$
$$M_{ss\ jj} = m_{s\ ij} \quad \& \ M_{ss\ aj} = 0 \ \ (that\ a \neq j) \tag{2}$$

$$K_{pp\ ii} = k_{p\ ii} + \sum k_{s\ ij}$$
$$K_{pp\ ai} = k_{p\ ai}\ \&\ K_{pp\ ia} = k_{p\ ia}\ (that\ a \neq i)$$
$$K_{ps\ ij} = -k_{s\ ij}\ \&\ K_{ps\ ab} = 0 (that\ a \neq i\ or\ b \neq j) \tag{3}$$
$$[K_{ps}] = [K_{sp}]^T$$
$$K_{ss\ jj} = k_{s\ ij}\ \&\ K_{ss\ aj} = K_{ss\ ja} = 0\ \ (that\ a \neq j)$$

If we calculate the determinants of the characteristic equation assuming free vibration, the characteristic relationship of mode *r* of the coupled system is as follows:

$$[K_c]\{\varphi_r^*\} = \omega_{cr}^2 [K_c]\{\varphi_r^*\} \tag{4}$$

Here, $\{\varphi_{r^*}\}$ represents the modal vector in mode *r* with *n*+*m* rows. First, the *n*-th row of Equation (4) in mode *r* is as follows:

$$[K]\begin{Bmatrix}\varphi_{1r}^{*}\\ \varphi_{2r}^{*}\\ \vdots\\ \varphi_{nr}^{*}\end{Bmatrix}+\{k_s\varphi^{*}\}=\omega_{cr}^{2}[M]\begin{Bmatrix}\varphi_{1r}^{*}\\ \varphi_{2r}^{*}\\ \vdots\\ \varphi_{nr}^{*}\end{Bmatrix} \tag{5}$$

The vector $\{k_s\varphi^*\}$, which has *n* rows, represents the effect of the secondary system on the characteristic equation of the primary system. If the *j*-th secondary system is connected to the *i*-th DOF, then the *i*-th member of this vector in the *r*-th mode equals $k_s\ i(\varphi_{ir}{}^*-\varphi_{n+1r}{}^*)$, and the rest of the members are zero. Therefore, the *i*-th member of the vector $\{k_s\varphi^*\}$ in the *r*-th mode is equal to:

$$\frac{m_{sj}\varphi_{ij}^{*}\omega_{cr}^{2}\omega_{sj}^{2}}{\omega_{cr}^{2}-\omega_{sj}^{2}} \tag{6}$$

If the mass of the secondary system is negative, then the value of this equation is small and can be neglected, except when the frequency of the secondary system is close to that of the primary structure. In addition, based on Rayleigh's quotient hypothesis, a first-order error in the mode shapes causes a second-order error in the frequency. Therefore, the hypothesis of the proximity of the first mode shapes of the primary and coupled structures caused a small error in the frequency and period calculations. Therefore, we simplified Equation (4) for the first mode.

$$\omega_p^2M_1+\sum_{l=1}^{m}m_{sl}\varphi_{j1}^{2}\frac{\omega_c^2\omega_{sl}^2}{\omega_c^2-\omega_{sl}^2}=\omega_c^2M_1 \tag{7}$$

Here, ω_p is the frequency of the first mode of the primary system, and ω_c is the frequency of the first mode of the coupled system. To functionalize the above relationship, with a simplified assumption, we assume that all the different frequencies of the secondary systems can be equated with an effective frequency equal to ω_{se}. If we replace the ω_{sl} in Equation (7) with the constant value ω_{se}:

$$\omega_p^2M_1+\frac{\omega_c^2\omega_{se}^2}{\omega_c^2-\omega_{se}^2}\sum_{l=1}^{m}m_{sl}\varphi_{j1}^{2}=\omega_c^2M_1 \tag{8}$$

By replacing the period with the frequency and simplifying Equation (8), we obtain:

$$\frac{{T_p}^4}{{T_c}^4}-\left(\frac{{T_p}^4}{{T_c}^2{T_{se}}^2}\right)\left(1+\frac{\sum m_{sr}\varphi_{r1}^2}{M_1}\right)+\frac{{T_p}^2}{{T_{se}}^2}-\frac{{T_p}^2}{{T_c}^2}=0 \tag{9}$$

Here, M_1 is the lumped mass of the primary system in the first mode.

$$M_1=\{\varphi_1\}^T[M]\{\varphi_1\}=\sum_{l=1}^{n}m_{pl}\varphi_{l1}^2 \tag{10}$$

In regular structures, the shape functions can be expressed as sine functions. By extending the power series of these sine functions and neglecting all expansion sentences except the first, the shape of the first mode becomes a simple linear function that is proportional to the height of the structure. Based on this simplified assumption, Equation (10) becomes the final equation:

$$\begin{gathered}{F_T}^4-\left({f_T}^2+\acute{\gamma}\right){F_T}^2+{f_T}^2=0\\ F_T=\frac{T_c}{T_p}\ \&\ f_T=\frac{T_{se}}{T_p}\ \&\ \gamma'=1+\gamma=1+\frac{\sum(m_sh_s^2)}{\sum(m_ph_p^2)}\end{gathered} \tag{11}$$

where F_T is the ratio of the coupled system period to the primary system period, f_T is the ratio of the secondary system period to the primary system period, and γ is the mass correction ratio. This relationship is similar to the coupled system with a secondary system relationship, with the difference that the definitions of the mass ratio and secondary system period have been changed in this relationship and have been defined more comprehensively for the multiplicity of secondary systems.

When calculating Equation (11), it was assumed that all different periods of the secondary systems could be equated with one effective period. As a result, the values of T_{se} and γ must be determined to express the effects of all secondary systems. The effect of each of these parameters on the coupled system period must be examined for this purpose.

To better investigate the effect of γ on the period of the coupled system, the value of F_T versus values of f_T were calculated in five mass percentage states for 0,0001; 0,010; 0,1000; 0,2500; and 1,0000; as presented in Figure 2.

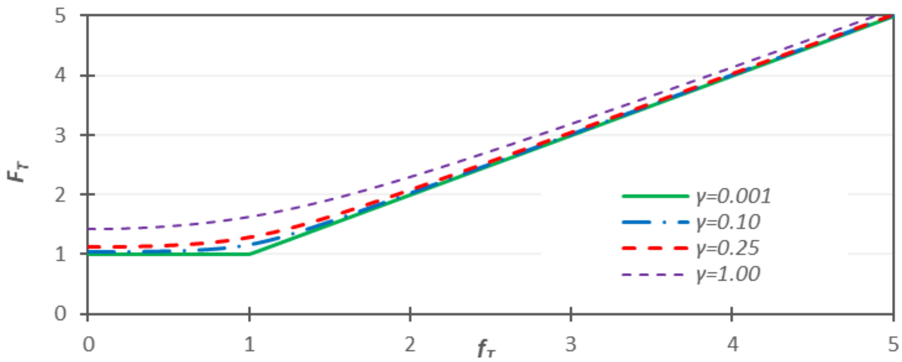

Figure 2. Variations of F_T versus f_T in terms of different mass ratios

Figure 2 shows that the F_T values did not increase much until f_T = 1. However, after f_T = 1, the coupled system period increased further, and the relationship between F_T and f_T tended to a linear relationship. Also, by increasing the f_T, the difference between the diagrams with the different mass ratios decreased. These results show that increasing the f_T results in the mass ratio having a lesser effect on the coupled system period. To better understand this issue, we calculated the F_T changes at different γ values compared with the F_T value at γ = 1,00 and 0,25; as shown in Figure 3.

Figure 3 shows that the effect of the mass ratio on the period of the coupled system exhibits an increasing trend until f_T reaches 1. After f_T=1, the effect of mass ratio decreases with a larger f_T such that after f_T = 3, the F_T change between different mass ratios is less than 5 %. The major change of FT is observed between the two states of γ = 0,0001 and γ = 1,00 at fT = 1, which has a value of less than 40 %. In conclusion, the main factor in determining the period of a coupled system is the f_T, and the effect of γ is much less than f_T. Also, as the value of f_T becomes larger than 1, the effect of γ on F_T decreases. Therefore, it can be assumed that the coupled system period is affected by the period of the secondary system connected to the primary structure that, if implemented alone, had the greatest effect on the coupled system period compared with other secondary systems. Owing to the lesser effects of the periods of the other secondary systems, the primary system period can be changed as a secondary mass. To identify the effective secondary period, each of the secondary systems should be added to the primary system, and the F_T value can be calculated for each of them separately via Equation 11. The secondary system with the maximum F_T is selected as the effective secondary system, and its period is set as T_{se}.

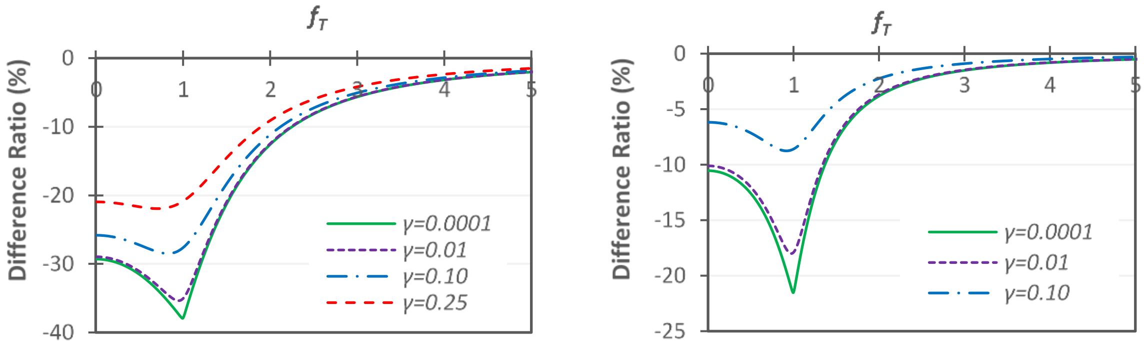

a) Baseline mass ratio equals 1,00 b) Baseline mass ratio equals 0,25

Figure 3. Difference ratios of F_T versus different mass ratios

The other secondary system periods do not affect the coupled system period, but their masses must be added to the mass ratio such that it appears to differ from the mass of the effective secondary system. According to Figure 3, if $f_{Te} \geq 3$, then we can ignore the mass effects of other secondary systems with a reasonable error percentage. If $f_{Te} < 3$, then we should calculate the equivalent secondary mass for inefficient secondary systems. If we calculate the values of the mass ratio from Equation (11), then:

$$\gamma = \frac{{F_T}^4 + {f_T}^2}{{F_T}^2} - \left({f_T}^2 + 1\right) \tag{12}$$

To make an equivalent secondary system from an effective secondary system, two γ terms are calculated from Equation (12), considering that their effects are constant. Then, Equation (13) can be obtained by calculating the discrepancy.

$$\gamma_i{}^* = \gamma_i - \left({f_{Te}}^2 - {f_{Ti}}^2\right)\left(1 - \frac{1}{{F_{Ti}}^2}\right) \tag{13}$$

The value of F_T always exceeds 1. Therefore, if $f_{Te} > f_{Ti}$, then the second part of Equation (13) becomes negative. As a result, $\gamma_{i^*} < \gamma_i$, and it is even possible that the γ_{i^*} value becomes negative. Accordingly, considering that the mass ratio has a lower effect than does the period, the result is achieved via a simplifying assumption. However, if the period of a secondary system in a coupled system is smaller than the effective secondary period, then its periodic and mass effects can be completely neglected. In addition, if $f_{Te} \leq f_{Ti}$, then the mass ratio of the ineffective secondary system must be calculated from Equation (13) and added to the mass ratio of the effective secondary system. Moreover, considering the lesser effect of the mass ratio compared with that of the period, we neglect the second part of Equation (13) and assume the value of γ_{i^*} equal to γ_i through another simplifying assumption. That is, the secondary system period in a coupled system is greater than the effective secondary period, its periodic effects are neglected, and only its mass ratio is added to the mass ratio of the effective secondary system. Therefore, Equation (14) is proposed as a design technique.

$$\begin{gathered} {T_{cr}}^2 = \frac{{T_p}^2}{2}\left(\alpha + \sqrt{\alpha^2 - 4{f_T}^2}\right) \\ \alpha = {f_T}^2 + \gamma_r + 1 \quad {f_T}^2 = \frac{{T_{sr}}^2}{{T_p}^2} \quad \gamma_r = \frac{\sum_{l=1}^{m} w_{sr} h_{sl}^2}{\sum_{l=1}^{n} w_{pl} h_{pl}^2} \end{gathered} \tag{14}$$

The coupled-system period was calculated using Equation (14), with the difference that T_c, T_{se}, and γ_{e^*} replace T_{cr}, T_{sr}, and γ_r, respectively (Equations (15) and (16)).

$$T_c{}^2 = \frac{T_p{}^2}{2}\left(\alpha + \sqrt{\alpha^2 - 4f_T{}^2}\right)$$
$$\alpha = f_T{}^2 + \gamma_e{}^* + 1 \qquad f_T{}^2 = \frac{T_{se}{}^2}{T_p{}^2} \tag{15}$$

$$T_{se} = T_{sr} \,\&\, \gamma_e = \gamma_r \;(that \;\; T_{cr} = max(T_{ci}))$$
$$if\;(f_{Te} \geq 3) \;\rightarrow\;\; \gamma_e{}^* = \gamma_e$$
$$if\;(f_{Te} < 3) \;\rightarrow \gamma_e{}^* = \gamma_e + \sum_{l=1}^{r} \gamma_l \;(if\; T_{sl} > T_{se}) \tag{16}$$

2.2 Comparison of the proposed analytical approach with existing models and codes of practice

As previously discussed, the PSSI is among the most important parameters in the analysis of secondary systems. Accordingly, the methods for analysing secondary systems can be examined using two approaches: (i) methods that do not consider PSSI and (ii) methods that consider the effects of interactions. In the first approach, the primary system is initially analysed without considering the secondary system, and the acceleration response of the structure is obtained at the support of the secondary system along its degrees of freedom. The response of the secondary system resulting from the effect of the structural response at the supports is then calculated. In the second approach, to consider PSSI, both primary and secondary systems must be modelled simultaneously as a composite system because the interaction affects the dynamic properties of the two systems and their response. If the secondary system has one SDOF, then the possibility of tuning must be considered. Otherwise, if the secondary system has an MDOF or multiple supports, then the effect of the correlation between the support motions must be considered.

The model proposed by Singh [24] does not consider this interaction, resulting in more conservative responses. In addition, if the frequency ratio of the two systems is close to 1 and the secondary-to-primary system mass ratio is large, then the estimation error in the frequency and system response increases. Gupta and Tembullkar [25] reported such results. According to Rayleigh's quotient hypothesis, the presence of a first-order error in the mode shape prompts a second-order error in the frequency. Therefore, the assumptions made in the model presented by Sackman et al. [26] caused a small error in frequency estimation. To overcome this shortcoming, Chen and Soong [27] proposed a model based on the NEHRP 1995 recommendations. Villaverde [28-32] recommended several simplified relations for analysing secondary systems. According to the method of Ghafouri and Fiouz [33] for calculating the response of secondary systems, if the connection of the secondary system to the primary structure is highly flexible, then the frequency of the secondary system tends to zero. Consequently, the acceleration of the secondary system becomes zero, although no force is applied, which is practically incorrect. Based on this premise, the relations presented in IBC 2006 have fundamental setbacks: (i) the equivalent static force recommended by the code is not correlated to the dynamic characteristics of the primary structure and is somehow independent of it, (ii) changes in the equivalent static force are assumed to be linear with the height of the structure, and (iii) the determination of the intensity coefficient, which indicates the degree of flexibility of the secondary system, is not sufficiently accurate.

In addition to the discussed models, Biggs and Roesset [34; 35] as well as Sackman and Kelly [36; 37] proposed a method that is widely used in practice. However, this method has several important drawbacks: (i) it is applicable only for secondary systems whose natural frequencies differ significantly from that of the primary structure, where the secondary system mass is small compared with that of the primary structure; (ii) it leads to unreasonable results for secondary systems with multiple supports. According to UBC 1997 [38], the force acting on nonstructural elements is calculated based on the ultimate strength, whereas the magnification factor of the secondary system can be obtained using the dynamic properties of the structure and secondary element. In addition, ASCE7-10 [39] reduced the magnification factor related to the location of the nonstructural element from 0,2-0,3. Based on the requirements of New Zealand NZS4219 [40; 41], the seismic load imposed on the secondary systems was estimated using the static equivalent force. Furthermore, the relationship proposed in Eurocode 2008 [42] calculates the horizontal earthquake force based on the ultimate strength at the secondary system mass centre in the direction with the greatest effect. Comprehensive research on the estimation of the fundamental period can be found in [43-45].

Accordingly, the seismic calculation methods and responses of secondary systems in most codes are based on equivalent seismic lateral force estimation. The force is directly proportional to the weight of the secondary system. However, in the case of secondary systems with multiple supports, there are practically no relationships or specific seismic conditions in these codes, and only displacement control of the supports is proposed. That is, PSSI has been ignored thus far because of the complexity of the relationships in secondary systems and the interaction conditions between the primary and secondary systems. As such, the calculation and design of these systems have been considered independently in current methods and standards. In addition, the location of the secondary system at the roof level is not considered in existing codes and standards. The relationships proposed in this study address the drawbacks of the existing methods used in seismic design.

2.3 Numerical approach

Several 3D moment-resisting frame structures with one, two, and three storeys, each consisting of four perimeter columns and four perimeter beams at each storey, were modelled using SAP200 software v.19 [46] as primary systems (Figure 1). In these models, the columns and beams comprised box sections with dimensions of 150 × 150 mm. In addition, each floor was modelled with a 5 mm thick steel plate with material specifications similar to those of the other steel materials. The height of each frame storey along the vertical axis was 4500 mm, and the span along both horizontal axes was 4500 mm. Reinforcing bars with lengths of 400 mm and diameters of 6 mm were attached to the primary system and used to model secondary systems with an overall mass of less than 20 % of that of the primary system.

To perform the finite element analysis, seven ground motion records obtained from PEER-NGA were selected and scaled in accordance with ASCE7-16 recommendations to represent a wide range of amplitudes (Tables 1 and 2).

It is worth noticing that the weight of each secondary system, per se, was 0,3 % of the primary system weight, which is quite negligible. The rebar models were tied to the frame floor at different locations on each floor in various configurations, although they exhibited similar stiffness and other seismic specifications.

Regarding the selection of records, Moeindarbary and Taghikhani [47] confirmed that the optimal design variables in the three levels of service-level earthquake (SLE), design-basis earthquake (DBE), and maximum considered earthquake (MCE) have similar characteristics; hence, hazard levels play no significant role in the selection procedure. A nonlinear dynamic time-history analysis was performed as part of the analysis step. Then, to compare the seismic response of the coupled system period with that obtained from the analytic approach, diagrams demonstrating the percentage differences between the associated responses were plotted versus variations in the mass ratio (γ). The steel material was ordinary structural steel with an elastic modulus of 200 GPa, yield stress of 240 MPa, and Poisson's ratio of 0,3. In addition, a bilinear model featuring strain hardening capacity was applied to simulate the nonlinear and inelastic properties of the steel material. As such, the plastic strain varied from a yield strain of 0,6 to the ultimate strain. The wall material was modelled as brick tiles with an elastic modulus of 1448 MPa, compressive strength of 2,5 MPa, and Poisson's ratio of 0,3. The concrete damage plasticity (CDP) was used to model the fracture behaviour of the bricks. Table 3 presents the damage variables assumed in the CDP model.

Table 1. Specifications of input ground motion records

ID No.	Earthquake			Recording station	Record seq. no.	Lowest freq. (Hz)	PGA (g)	PGV (cm/sec)
	M	Year	Name					
1	6,7	1994	Northridge	Beverly Hills - Mulhol	953	0,25	0,52	63
2	7,1	1999	Duzce,Turkey	Bolu	1602	0,06	0,82	62
3	6,9	1995	Kobe,Japan	Nishi-Akashi	1111	0,13	0,51	37
4	7,3	1992	Landers	Coolwater	848	0,13	0,42	42
5	6,9	1989	Loma Prieta	Capitola	752	0,13	0,53	35
6	7,4	1990	Manjil,Iran	Abbar	1633	0,13	0,51	54
7	7,6	1999	Chi-Chi,Taiwan	TCU045	1485	0,05	0,51	39

Table 2. Scale factors for the ground motion excitations in the preliminary analysis step

ID No.	Earthquake	Scaling factor
1	Northridge	0,7941
2	Duzce, Turkey	1,0405
3	Kobe, Japan	0,6996
4	Landers	0,6406
5	Loma Prieta	0,6509
6	Manjil, Iran	1,0971
7	Chi-Chi, Taiwan	1,0171

Table 3. Damage variables assumed in CDP model

Ψ	ε	f_{b0}/f_c	K_c	μ
40	0,100	1,160	0,670	0,001

All the modelled primary and coupled frame structures were initially examined via modal analysis, and the associated fundamental periods were accurately computed using software. Therefore, the coupled system period was calculated using Equations (14)-(16). Furthermore, the discrepancy between the proposed relationship for the coupled structural period and that obtained from the numerical analysis was compared.

Considering the complexity of the dynamic relationships between the primary and secondary systems, in previous studies that have been the basis of design code relationships, the interaction effects of the primary and secondary systems have been neglected, and secondary systems have only been applied as masses on primary structures. Therefore, in the numerical part of this study, an attempt was made to provide a simple design technique for the calculation of the fundamental period of a coupled system, considering the multiplicity of secondary systems, by completing previous research and developing and simplifying the dynamic relationships. Consequently, the fundamental period of the coupled structure replaces the period of the primary structure in seismic design relationships and techniques.

3 Results and discussion

In this section, the periods of the coupled systems resulting from the combination of a single-degree-of-freedom primary system with 1, 2, 10, and 20 secondary systems are calculated according to the results obtained from both numerical modelling and the proposed analytical relationship. The periods of the modelled frame structures obtained from SAP200 are shown in the following figures. Accordingly, the secondary systems were modelled with different stiffness values, as denoted by SS1-SS5 in the figure legends. The stiffness of the secondary systems increases from SS1 to SS5.

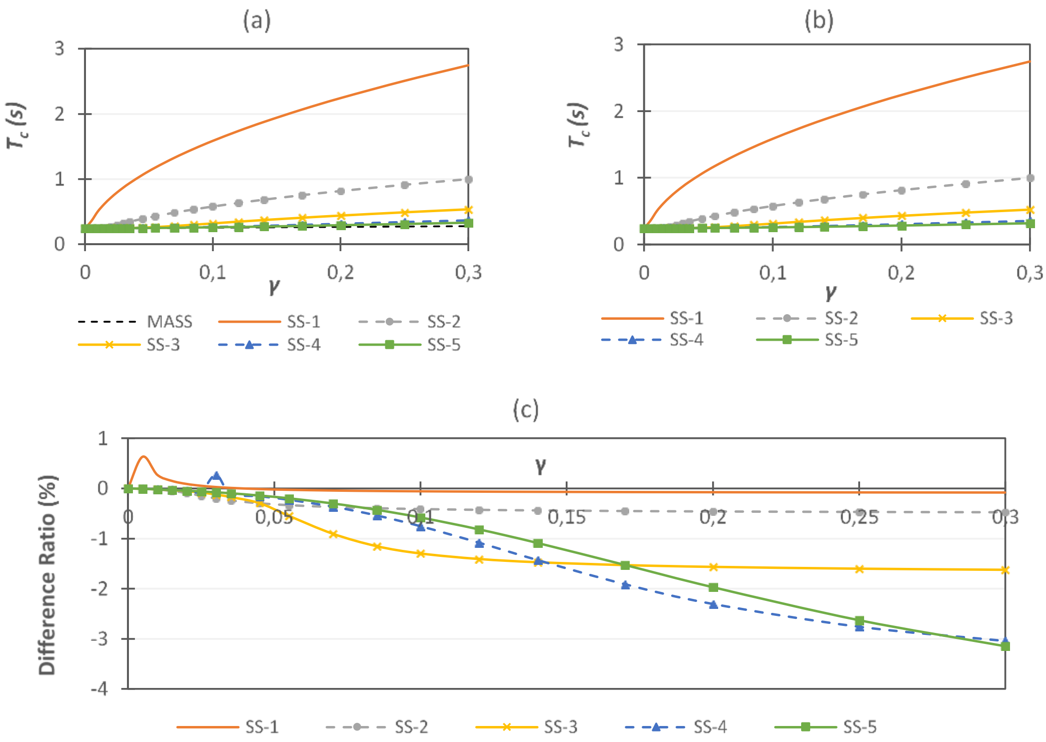

Figure 4. Variations of the fundamental periods of one-storey frame structures coupled with one secondary system versus the mass ratio (γ) obtained via: a) numerical analysis, b) the proposed relation, and c) the difference ratio $T_{c-equation}/(T_{c-software}-1)$

According to Figure 4, the fundamental period of the one-storey frame structure coupled with one secondary system increases with an increasing mass ratio (γ) in both approaches. Based on the diagrams shown in Figures 4a) and b), the increasing trend of the period is similar for both the numerical and analytical methodologies. Moreover, increasing the stiffness of the secondary system reduces the period of the coupled primary–secondary structures.

The difference ratios between the numerical and proposed analytical methods are plotted in Figure 4c). Based on this figure, the difference ratio ($T_{c-equation}/T_{c-software}-1$) typically increases with an increasing mass ratio (γ). This discrepancy was the lowest when the stiffness of the secondary system was the lowest. Thus, the periodic ratio increased when the secondary system stiffness increased.

The fundamental periods of the one-storey frame structure coupled with two secondary systems are demonstrated versus the mass ratio (γ), regarding different secondary system stiffness values in Figure 5. The variation trends of the coupled system periods in the numerical and analytical approaches are similar. Therefore, the period of the coupled system increases in both approaches as the mass ratio increases. Furthermore, an increase in the stiffness of the secondary system decreased the period of the coupled system.

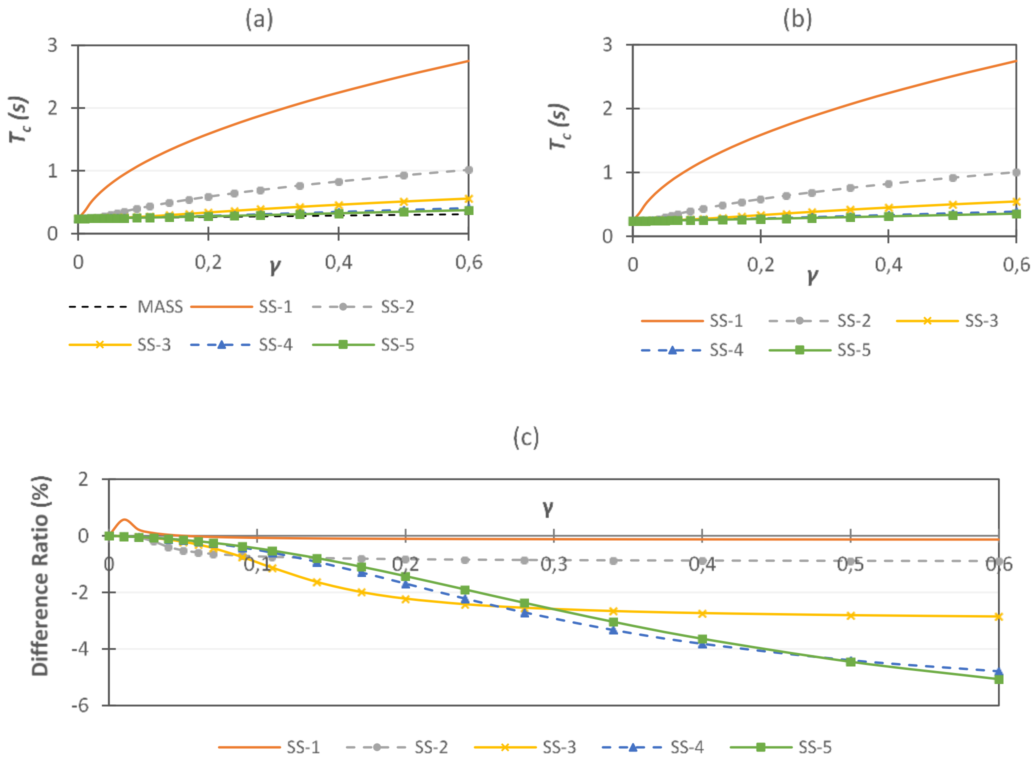

Figure 5. Variations of the fundamental periods of a one-storey frame structure coupled with two secondary systems versus the mass ratio (ɣ) obtained via: a) numerical analysis, b) the proposed relation, and c) the difference ratio $T_{c\text{-}equation}/T_{c\text{-}software}$-1

Likewise, Figure 6 shows the fundamental period of a single-storey frame structure coupled with 10 secondary systems against different mass ratios (ɣ). According to this figure, the greatest system period is associated with the secondary system with the lowest value, that is, SS1. Therefore, the coupled system period in both methods decreased as the stiffness of the secondary system increased. Additionally, the difference in the system period between the two approaches was the lowest in the system with the lowest secondary system stiffness.

The fundamental period of a single-storey frame structure coupled with 20 secondary systems against different mass ratios (ɣ) is plotted in Figure 7. The same variation trend holds true for the system period with 20 secondary systems having different stiffnesses compared with systems with fewer attached secondary systems. These results can be observed in Figure 7, which shows that the period discrepancy between the two approaches increases with an increase in the number of secondary systems.

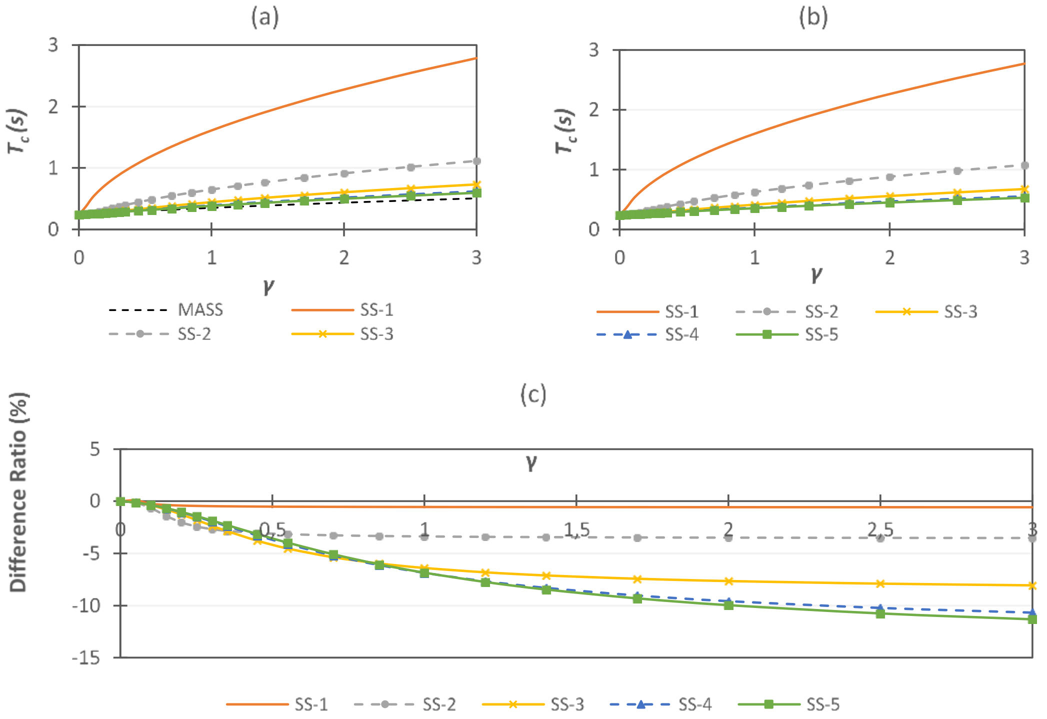

Figure 6. Variations of the fundamental periods of a one-storey frame structure coupled with 10 secondary systems versus the mass ratio (ɣ) obtained via: a) numerical analysis, b) the proposed relation, and c) the difference ratio $T_{c\text{-}equation}/T_{c\text{-}software}$-1

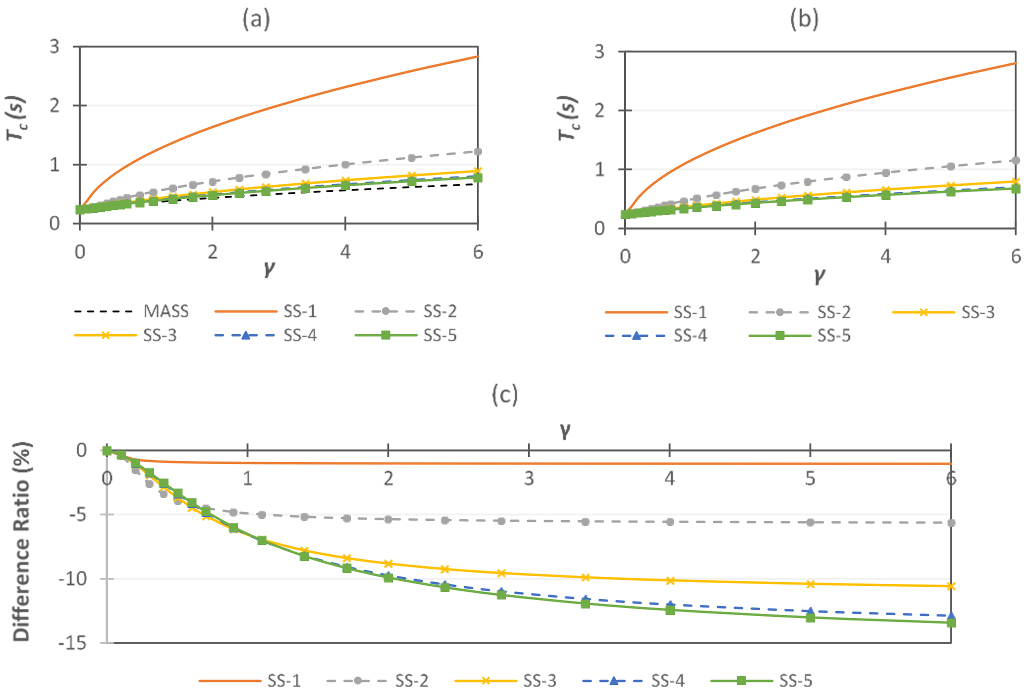

Figure 7. The variations of fundamental periods of a one-storey frame structure coupled with 20 secondary systems versus the mass ratio (ɣ) obtained via: a) numerical analysis, b) the proposed relation, and c) the difference ratio $T_{c\text{-}equation}/T_{c\text{-}software}$-1

The diagrams above indicate that in cases of single-storey coupled frame structures, where the number of secondary systems is low, the difference between the results obtained from the proposed relationship and those given by the numerical analysis is less because of the small mass ratio of the secondary systems. However, the two method results begin to diverge as the number of secondary systems increased. Consequently, the mass ratio (γ) increases. This trend could be investigated from two perspectives. First, as is evident in all diagrams, the difference ratios for the proposed relationship are negative. That is, the approximate proposed relationship always results in values that are lower than the actual values, which should be a matter of the safety margin in the calculations. Second, as acknowledged for conventional building structures, the mass ratio of the entire secondary system to the primary system is typically low, with values being less than 1 and generally less than 0,5. Nevertheless, the difference in the period between the proposed relationship and numerical study was lower than 5 %, which is admissible.
Notably, in some diagrams, the value of γ takes on numbers greater than one. These outcomes resulted because, in the selection of the secondary system, its mass was set to be at most 30 % of that of the storey. For a better comparison of the effects of multiple secondary systems on the periods of coupled systems, in the current seismic codes of practice, this mass ratio is kept constant for each secondary system with an increasing number of secondary systems. Thus, given that the primary and secondary systems were assumed to be independent of each other, the maximum mass of each secondary system was limited to 25 % of that of the primary structure. Therefore, if each secondary system satisfies this limit, no particular measures are required, even if the total number of secondary systems exceeds this limit. However, the results of this study confirm that the multiplicity of the secondary systems plays a major role in the determination of the fundamental period of the coupled system, given that the primary–secondary system interactions are considered.
In accordance with the results obtained for the fundamental period of the coupled frame structures with two degrees of freedom (two storeys), the variation trend of the system period with respect to different mass ratios was similar to that already discussed for systems with a single degree of freedom. An example of a two-storey frame is presented here. According to Figure 8, the fundamental period of a two-storey frame structure coupled with 20 secondary systems against different mass ratios (γ) is demonstrated, in which all 20 secondary systems are modelled on the second floor. The greatest system period was related to the secondary system with the lowest value (i.e., SS1). Therefore, the coupled system period in both methods decreased as the stiffness of the secondary system increased. Additionally, the difference in the system period between the two approaches was the lowest in the systems with the lowest secondary system stiffness. Nevertheless, in structures in which all multiple secondary systems were on the first floor, a higher discrepancy was observed between the two approaches, although the rate of difference was still less than 10 %.
The same was applied to frame structures with three storeys. Consequently, it was observed that the variation trend of the system period with respect to different mass ratios was analogous to that observed for systems with a single degree of freedom. Thus, an instance of a three-storey frame was investigated as follows. Based on Figure 9, the fundamental period of a three-storey frame structure coupled with 10 secondary systems against different mass ratios (γ) are established. In principle, the highest value of the system period corresponded to the lowest stiffness value of the secondary system. Consequently, the coupled system period in both methods decreased as the secondary system stiffness increased. Moreover, the difference in the system period between the two approaches was the lowest in the systems with the lowest secondary system stiffness.

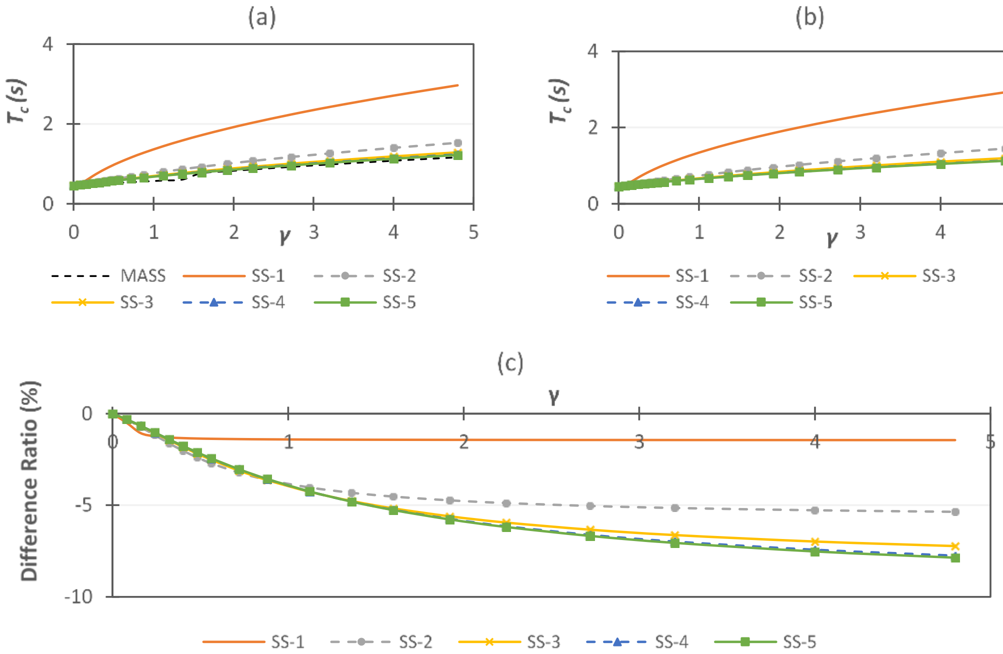

Figure 8. Variations of the fundamental periods of a two-storey frame structure coupled with 20 secondary systems versus the mass ratio (γ) obtained via: a) numerical analysis, b) the proposed relation, and c) difference ratio $T_{c\text{-}equation}/T_{c\text{-}software}$-1

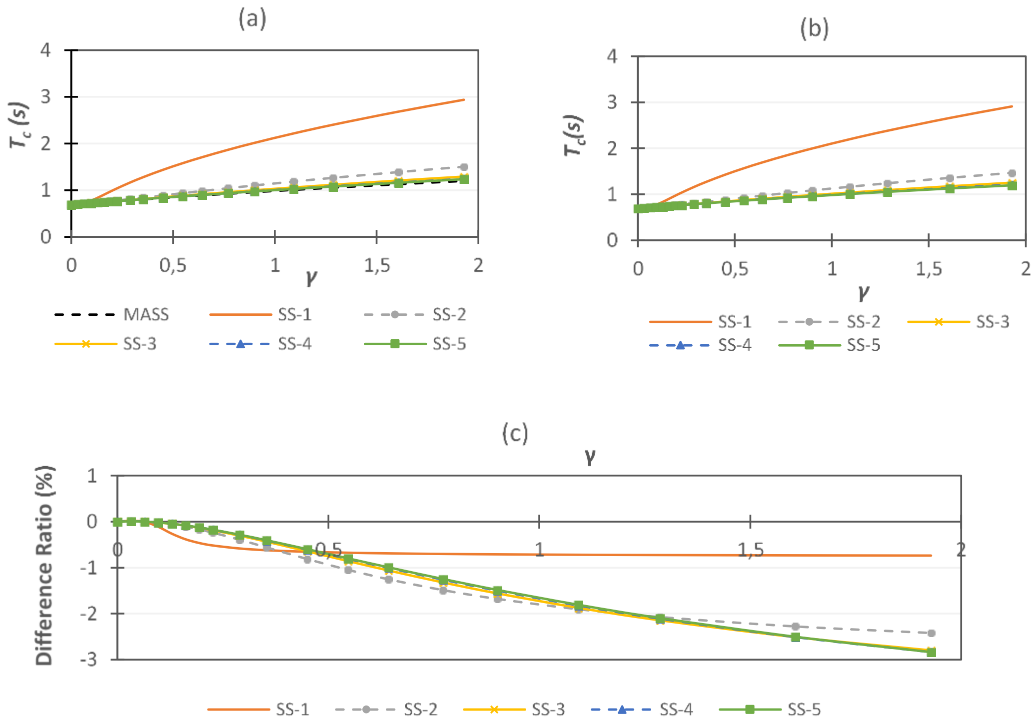

Figure 9. Variations of the fundamental periods of a three-storey frame structure coupled with 10 secondary systems versus the mass ratio (γ) obtained via: a) numerical analysis, b) the proposed relation, and c) the difference ratio $T_{c\text{-}equation}/T_{c\text{-}software}$-1

The overall examination of structures with three degrees of freedom also indicates that the proposed relationship has acceptable accuracy for use as a design technique by engineers and practitioners. This relationship (Equations (14)-(16)) can predict the period of the coupled system with acceptable accuracy when the secondary systems are distributed over all floors. In addition to the fact that the error of the proposed equation in this study is still less than 5 % in the range of the actual measures of the mass ratios (γ) in conventional structures (which are less than 0,5); the errors generally fall in line with the safety factor, thus demonstrating the feasibility of the proposed relation.

Moreover, the investigation of the diagrams of different structures shows that by increasing the degrees of freedom of the primary structure, the amount of the mentioned error in similar situations decreases, which is attributable to the better distribution of masses at the height. Another important point to note is that for equal mass measures, the longer the period of the secondary system increases compared with other secondary systems, the more the computation error increases.

In addition, the analysis of the diagrams shows that the main parameter in the variation of the period of the primary system is the period of the secondary system. Thus, if the secondary system period is shorter than that of the primary system, the effects of the secondary system period can be ignored.

Finally, by using the coupled system period instead of the primary system period, seismic design errors can be reduced by ignoring secondary systems. It may also be possible to increase the periods of short-period structures under the effects of secondary system periods via the periodic and mass potentials of the secondary systems to thereby improve their seismic behaviours.

4 Conclusion

In the present study, numerical and analytical investigations were carried out to estimate the fundamental periods of coupled primary-secondary structural systems. Therefore, a number of 3D steel moment-resisting frame structures with one, two, and three storeys, each of which comprised four perimeter columns and four perimeter beams at each storey, were modelled using SAP2000 software v.19 as primary systems to assess the effects of secondary system multiplicity, the distribution of secondary systems on different storeys, and the number of storeys (degrees of freedom) on the period of the coupled structure. The following conclusions were drawn from the findings:

- Despite the low masses of the secondary systems, the period of the coupled system changed significantly with the addition of secondary systems to the primary structure.
- The most significant effect of the secondary system on the response of the coupled system is the structural period in the design procedure.
- The proposed approach has the advantage of modifying the period of primary structures with lower values so that the coupled structure would benefit from increased period values by using the potential of multiple secondary systems.
- The fundamental period of the one-storey frame structure coupled with one secondary system increases with an increasing mass ratio (γ) in both numerical and analytical approaches. Similar trends have been observed for systems with higher degrees of freedom.
- Increasing the stiffness of the secondary system reduces the period of the coupled primary–secondary structures.
- The periodic difference ratio ($T_{c\text{-}equation}/T_{c\text{-}software}$-1)) typically increased with an increasing mass ratio (γ). This discrepancy was the lowest when the stiffness of the secondary system was the lowest. The periodic difference ratio increased with the secondary system stiffness.
- The difference between the results obtained from the proposed relationship and those obtained via numerical analysis was small because of the small mass ratio of the secondary systems. However, the results of the two methods diverged as the number of secondary systems increased.

- If the secondary system period is shorter than that of the primary system, the effects of the secondary system period can be ignored.
- Using the coupled system period instead of the primary system period can significantly reduce the seismic design errors arising from ignoring secondary systems. It may also be possible to increase the period of short-period structures under the effect of the secondary system period via the periodic and mass potential of the secondary systems, to thereby improve their seismic behaviours.
- With increasing degrees of freedom of the primary structure, the magnitude of the mentioned error in similar situations decreases. These results are attributable to the better distribution of masses at the height.

Abbreviations

PSSI	primary-secondary system interactions
MDOF	multi degrees-of-freedom
MRF	moment-resisting frame
i index	degree of freedom of the primary system
j index	degree of freedom of the secondary system
SDOF	single degree-of-freedom
ms ij	mass of the *j*-th secondary system, connected to *i*-th degree of freedom in the primary system
ks ij	stiffness of the *j*-th secondary system, connected to *i*-th degree of freedom in the primary system
$[M_p]$	mass matrix of the primary system
$[K_p]$	stiffness matrix of the primary system
$[M_c]$	mass matrix of the coupled system
$[K_c]$	stiffness matrix of the coupled system
$\{\varphi_{r^*}\}$	modal vector in mode *r*
$\{k_s\varphi^*\}$	secondary system's effect vector on the primary system
ω_p	frequency of the first mode of the primary system
ω_c	frequency of the first mode of the coupled system
ω_{se}	effective frequency of the secondary systems
F_T	ratio of the coupled system period to the primary system period
f_T	ratio of the secondary system period to the primary system period
γ	mass correction ratio
$T_{c\text{-}equation}$	fundamental period obtained via analytical approach
$T_{c\text{-}software}$	fundamental period obtained via numerical approach
3D	three-dimensional
SAP	structural analysis program
PEER-NGA	pacific earthquake engineering research
ASCE	American society of civil engineering
PGA	peak ground acceleration
PGV	peak ground velocity
SLE	service level earthquake
DBE	design basis earthquake
MCE	maximum considered earthquake
γ	mass ratio
CDP	concrete damage plasticity
SS	Secondary system

References

[1] Caicedo, D.; Lara-Valencia, L.; Blandon, J.; Graciano, C. Seismic response of high-rise buildings through metaheuristic-based optimization using tuned mass dampers and

tuned mass dampers inerter. *Journal of Building Engineering*, 2021, 34, 101927. https://doi.org/10.1016/j.jobe.2020.101927

[2] Dhakal, R. P. et al. 2016. Seismic performance of non-structural components and contents in buildings: an overview of NZ research. *Earthquake Engineering and Engineering Vibration*, 2016, 15, pp. 1-17. https://doi.org/10.1007/s11803-016-0301-9

[3] Butenweg, C. et al. Seismic performance of an industrial multi-storey frame structure with process equipment subjected to shake table testing. *Engineering Structures*, 2021, 243, 112681. https://doi.org/10.1016/j.engstruct.2021.112681

[4] Yang, T. Y.; Qiao, T.; Tobber, L.; Rodgers, G. W. Seismic performance of controlled outrigger rocking wall system with different energy dissipation devices. *Soil Dynamics and Earthquake Engineering*, 2022, 155, 107179. https://doi.org/10.1016/j.soildyn.2022.107179

[5] Perrone, D. et al. Seismic performance of non-structural elements during the 2016 Central Italy earthquake. *Bulletin of Earthquake Engineering*, 2019, 17, pp.5655-5677. https://doi.org/10.1007/s10518-018-0361-5

[6] Ghafoori-Ashtiani, M.; Foyooz, A. Absolute Acceleration Transfer Function of Secondary Systems Subjected to Multi-Component Earthquakes. *Journal of Advanced Materials in Engineering (Esteghlal)*, 2022, 21 (1), pp.113-139.

[7] Butenweg, C. et al. Experimental investigation on the seismic performance of a multi-component system for major-hazard industrial facilities. In: *Pressure Vessels and Piping Conference*. July 13-15, 2021, Virtual, Online, American Society of Mechanical Engineers; 2021. https://doi.org/10.1115/PVP2021-61696

[8] Ryan, K. L. et al. Seismic simulation of an integrated ceiling-partition wall-piping system at E-Defense. I: Three-dimensional structural response and base isolation. *Journal of Structural Engineering*, 2015, 142 (2), 04015130. https://doi.org/10.1061/(ASCE)ST.1943-541X.0001384

[9] Adam, C. Dynamics of elastic-plastic frames with secondary structures: shake table and numerical studies. *Journal of Earthquake Engineering & Structural Dynamics*, 2001, 30 (2), pp. 257-277. https://doi.org/10.1002/1096-9845(200102)30:2%3C257::AID-EQE7%3E3.0.CO;2-J

[10] Filiatrault, A.; Perrone, D.; Merino, R. J.; Calvi, G. M. Performance-based seismic design of nonstructural building elements. *Journal of Earthquake Engineering*, 2021, 25 (2), pp. 237-269. https://doi.org/10.1080/13632469.2018.1512910

[11] Merino, R. J.; Perrone, D.; Filiatrault, A. Consistent floor response spectra for performance-based seismic design of nonstructural elements. *Journal of Earthquake Engineering & Structural Dynamics*, 2019, 49 (3), pp. 261-284. https://doi.org/10.1002/eqe.3236

[12] Surana, M. Evaluation of seismic design provisions for acceleration-sensitive nonstructural components. *Earthquakes and Structures*, 2019, 16 (5), pp. 611-623. https://doi.org/10.12989/eas.2019.16.5.611

[13] Kazantzi, K. A.; Miranda, E.; Vamvatsikos, D. Strength-reduction factors for the design of light nonstructural elements in buildings. *Earthquake Engineering & Structural Dynamics*, 2020, 49 (13), pp. 1329-1343. https://doi.org/10.1002/eqe.3292

[14] Chalarcal, B.; Filiatrault, A.; Perrone, D. Seismic demand on acceleration-sensitive nonstructural components in viscously damped braced frames. *Journal of Structural Engineering*, 2020, 146 (9). https://doi.org/10.1061/(ASCE)ST.1943-541X.0002770

[15] Zhao, Q.; Qiu, J.; Zhao, Y.; Yu, C. Estimating Fundamental Period of Corrugated Steel Plate Shear Walls. *KSCE Journal of Civil Engineering*, 2020, 24, pp. 3023-3033. https://doi.org/10.1007/s12205-020-2305-2

[16] Jiang, R. et al. A simplified method for fundamental period prediction of steel frames with steel plate shear walls. *Structural Design of Tall and Special Buildings*, 2020, 29 (7), e1718. https://doi.org/10.1002/tal.1718

[17] Jiang, R. et al. A simplified method for estimating the fundamental period of masonry infilled reinforced concrete frames. *Structural Engineering and Mechanics*, 2020, 74 (6), pp. 821-832.

[18] De, M.; Sengupta, P.; Chakraborty, S. Fundamental periods of reinforced concrete building frames resting on sloping ground. *Earthquakes and Structures*, 2018, 14 (4), pp. 305-312. https://doi.org/10.12989/eas.2018.14.4.305

[19] Asteris, P. G. et al. Fundamental period of infilled R.C. frame structures with vertical irregularity. *Structural Engineering and Mechanics*, 2017, 61 (5), pp. 663-674.

[20] Charalampakis, A. E.; Tsiatas, G. C.; Kotsiantis, S. B. *Machine learning and nonlinear models for the estimation of fundamental period of vibration of masonry infilled R.C. frame structures*. *Engineering Structures*, 2020, 216, 110765. https://doi.org/10.1016/j.engstruct.2020.110765

[21] Pandian, A. V. P.; Vinu, M. Effects of Fundamental Natural Time Periods on the Seismic Performance of Base Isolated Multistory Buildings. *Asian Journal of Civil Engineering,* Ahead-of-Print. https://doi.org/10.21203/rs.3.rs-2512780/v1

[22] Asteris, P. G. Lateral stiffness of brick masonry infilled plane frames. *Journal of structural engineering*, 2003, 129 (8), pp.1071-1079. https://doi.org/10.1061/(ASCE)0733-9445(2003)129:8(1071)

[23] Yekrangnia, M.; Asteris, P. G. Multi-strut macro-model for masonry infilled frames with openings. *Journal of Building Engineering*, 2020, 32, 101683. https://doi.org/10.1016/j.jobe.2020.101683

[24] Singh, M. P. Seismic design input for secondary systems. *Journal of the Structural Division*, 1980, 106 (2), pp.505-517. https://doi.org/10.1061/JSDEAG.0005371

[25] Gupta, A. K.; Tembulkar, J. M. Dynamic decoupling of secondary systems. *Nuclear Engineering and Design*, 1984, 81 (3), pp. 359-373. https://doi.org/10.1016/0029-5493(84)90282-6

[26] Sackman, J. L.; Der Kiureghian, A.; Nour-Omid, B. Dynamic analysis of light equipment in structures: modal properties of the combined system. *Journal of Engineering Mechanics*, 1983, 109 (1), pp. 73-89. https://doi.org/10.1061/(ASCE)0733-9399(1983)109:1(73)

[27] Chen, Y.; Soong, T. T. Seismic response of secondary systems. *Engineering Structures*, 1988, 10 (4), pp. 218-228. https://doi.org/10.1016/0141-0296(88)90043-0

[28] Villaverde, R. Seismic design of secondary structures: state of the art. *Journal of Structural Engineering*, 1997, 123 (8), pp. 1011-1019. https://doi.org/10.1061/(ASCE)0733-9445(1997)123:8(1011)

[29] Villaverde, R. Simplified seismic analysis of secondary systems. *Journal of Structural Engineering*, 1986, 112 (3), pp. 588-604. https://doi.org/10.1061/(ASCE)0733-9445(1986)112:3(588)

[30] Villaverde, R. Simplified seismic analysis of piping or equipment mounted on two points of a multistory structure. *Nuclear Engineering and Design*, 1986, 92 (1), pp. 37-50. https://doi.org/10.1016/0029-5493(86)90097-X

[31] Villaverde, R. Simplified approach for the seismic analysis of equipment attached to elastoplastic structures. *Nuclear Engineering and Design*, 1987, 103 (3), pp. 267-279. https://doi.org/10.1016/0029-5493(87)90310-4

[32] Villaverde, R. Approximate formulas to calculate the seismic response of light attachments to buildings. *Nuclear Engineering and Design*, 1991, 128 (3), pp. 349-368. https://doi.org/10.1016/0029-5493(91)90172-E

[33] Ghafory-Ashtiany, M.; Fiouz, A. R. Response of Secondary Systems Subjected to Multicomponent Earthquake Input. *Journal of Seismology & Earthquake Engineering*, 2004, 6 (2), pp. 29-45.

[34] Biggs, J. M.; Roesset, J. M. 1970. Seismic analysis of equipment mounted on a massive structure. *Seismic Design for Nuclear Power Plants*, 1970, pp. 319-343.

[35] Biggs, J. M. Seismic response spectra for equipment design in nuclear power plants. In: *Proceedings of the first international conference on structural mechanics in reactor technology*. September 20, 1971, Berlin, Germany, 1971, pp. 329-343.

[36] Sackman, J. L.; Kelly, J. M. Rational design methods for light equipment in structures subjected to ground motion. Earthquake Engineering Research Center, University of California, Berkley, USA, 1978.

[37] Sackman, J. L; Kelly, J. M. Seismic analysis of internal equipment and components in structures. *Engineering Structures*, 1979, 1 (4), pp. 179-190. https://doi.org/10.1016/0141-0296(79)90045-2

[38] International Conference of Building Officials (ICBO). *Uniform Building Code, Chapter 16: Section 1632 – Lateral force on elements of structures, non-structural components and equipment supported by structures*. USA: ICBO; 1997.

[39] American Society of Civil Engineering Standard. ASCE/SEI 7-10. *Minimum Design Load for Buildings and Other Structures*. USA: ASCE; 2010.

[40] Standards New Zealand. NZS4219. *Seismic Performance of Engineering Systems in Buildings*. New Zealand: NZS; 2009.

[41] Standards New Zealand. NZS1170.5. *Structural Design Actions Part 5: Earthquake Action*. New Zealand: NZS; 2004.

[42] European tandard. EN 1998-1:2004. *Eurocode 8: Design of structures for earthquake resistance*. EU: EN; 2004.

[43] Asteris, P. G. et al. On the fundamental period of infilled RC frame buildings. *Structural Engineering and Mechanics*, 2015, 54 (6), pp. 1175-1200. https://doi.org/10.12989/sem.2015.54.6.1175

[44] Asteris, P. G.; Repapis, C. C.; Repapi, E. V.; Cavaleri, L. Fundamental period of infilled reinforced concrete frame structures. *Structure and Infrastructure Engineering*, 2017, 13 (7), pp. 929-941. https://doi.org/10.1080/15732479.2016.1227341

[45] Cavaleri, L.; Di Trapani, F.; Asteris, P. G.; Sarhosis, V. Influence of column shear failure on pushover based assessment of masonry infilled reinforced concrete framed structures: A case study. *Soil Dynamics and Earthquake Engineering*, 2017, 100, pp. 98-112. https://doi.org/10.1016/j.soildyn.2017.05.032

[46] Alami, F.; Khotimah, S. N. *Manual Structural Analysis Program (SAP) 2000*. Lampung Jurusan Teknik Sipil Universitas Lampung, 2017.

[47] Moeindarbari H.; Taghikhany T. Seismic optimum design of triple friction pendulum bearing subjected to near-fault pulse-like ground motions. *Structural and Multidisciplinary Optimization*, 2014, 50, pp. 701-716. https://doi.org/10.1007/s00158-014-1079-x